Macromolecular Bioscience
www.mbs-journal.de

High Molecular Weight Poly(ethylenimine)-Based Water-Soluble Lipopolymer for Transfection of Cancer Cells

*Heba Alaa Hosiny Abd Elhameed, Ditta Ungor, Nóra Igaz, Mohana Krishna Gopisetty, Mónika Kiricsi, Edit Csapó, and Béla Gyurcsik**

Over the past decade, search for novel materials for nucleic acid delivery has prompted a special interest in polymeric nanoparticles (NPs). In this study, the biological applicability of a water-soluble cationic lipopolymer (WSLP) obtained by the modification of high molecular weight branched poly(ethylenimine) (PEI) with cholesteryl chloroformate is characterized and assessed for better cellular membrane permeability. To test the delivery efficiency of the produced lipopolymer, plasmid DNA (pDNA) encoding the enhanced green fluorescent protein and WSLP are mixed at different charge ratios. WSLP and WSLP/pDNA complexes are characterized by dynamic and static light scattering, particle charge detection, scanning electron microscopy, and transmission electron microscopy. The pDNA loading of WSLP is also verified by agarose gel electrophoresis. Cytotoxicity of PEI, WSLP, and of WSLP/pDNA is evaluated on human A549 and HeLa cells. A remarkable dependence of the toxicity on the dose, cholesterylation, and charge ratio is detected. Transfection is monitored by flow cytometry and by fluorescence microscopy. Importantly, cholesterylation decreases the toxicity of the polymer, while promoting high transfection efficiency in both cell lines. This work indicates a possible optimization mode of the high molecular weight PEI-based WSLP rendering it a promising candidate for gene delivery.

1. Introduction

Gene therapy offers a potential cure for hereditary diseases. For effective clinical application, the development of competent gene delivery systems is essential.[1–4] To this date mainly two types of delivery approaches are available using either viral or non-viral vehicles. Viral vectors (adeno-associated virus and lentivirus) are efficient gene delivery systems but they have numerous limitations such as potential carcinogenesis, immunogenicity, limited DNA packaging size, and difficulty in production.[5] Non-viral vectors are preferred for gene delivery purpose because these systems have shown less side-effects.[6–9]

The widely used physical delivery methods applied with non-viral vehicles depend on creating a simple pierce in the cell membrane by electroporation, microinjection, induced transduction, mechanical cell deformation, and hydrodynamic injection. Thus, they are rather convenient for in vitro applications. Chemical vehicles such as lipid or polymeric nanoparticles, cell-penetrating peptides, DNA nanostructures, and gold nanoparticles hold enormous potential for in vivo applications. Cationic polymers such as poly(ethylenimine) (PEI), polylysine, amine-functionalized poly-caprolactone, and chitosan are widely used as gene carriers. These can be prepared easily and have a high DNA packaging ability at physiological pH.[10,11] Among them, PEI is one of the leading transfection reagents because of the high concentration of positively charged amino groups, interacting strongly with the negatively charged DNA, forming condensed DNA/PEI complexes, and ultimately protecting the genetic material from the enzymatic degradation.[12–14] The first application of PEI as transfection reagent was published in 1995.[15] Branched and linear PEIs have been utilized ever since to deliver nucleic acids both in vitro and in vivo.[16,17] PEI-based nanocarriers promote efficient transfection.[18–20] Modification

H. A. H. Abd Elhameed, Dr. B. Gyurcsik
Department of Inorganic and Analytical Chemistry
University of Szeged
Dóm tér 7, Szeged H-6720, Hungary
E-mail: gyurcsik@chem.u-szeged.hu

The ORCID identification number(s) for the author(s) of this article can be found under https://doi.org/10.1002/mabi.202000040.

DOI: 10.1002/mabi.202000040

Dr. D. Ungor, Dr. E. Csapó
Interdisciplinary Excellence Centre, Department of Physical Chemistry and Materials Science
University of Szeged
Rerrich Béla tér 1, Szeged H-6720, Hungary

Dr. E. Csapó
Faculty of Medicine
MTA-SZTE Biomimetic Systems Research Group
Department of Medical Chemistry
University of Szeged
Dóm tér 8, Szeged H-6720, Hungary

N. Igaz, M. K. Gopisetty, Dr. M. Kiricsi
Department of Biochemistry and Molecular Biology
Doctoral School of Biology
University of Szeged
Közép fasor 52, Szeged H-6726, Hungary

of PEI using different polymers and ligands has recently been widely studied to overcome the limitations of its application, such as the increasing cytotoxicity with increasing molecular weight and aggregation in the case of high ionic strength.[21–35]

Along this line, herein we used high molecular weight (HMW) branched PEI-based cationic water-soluble lipopolymer (WSLP) for non-viral gene delivery. Our system contained PEI primarily to enhance plasmid DNA (pDNA) condensation and its endosomal release due to its tertiary amines, and the cholesteryl groups served as the lipid component to increase the transport of pDNA through the cell membranes. The pDNA loading was monitored by physico–chemical methods, while the cytotoxicity and transfection efficiency were evaluated by a colorimetric assay based on 3-[4,5-dimethylthiazol-2-yl]-2,5-diphenyltetrazolium bromide (MTT assay) and by flow cytometry, as well as fluorescence microscopy based on the enhanced green fluorescent protein (EGFP) fluorescence, respectively.

2. Results and Discussion

2.1. Synthesis and Characterization of Water-Soluble Lipopolymer

WSLP was prepared from PEI and cholesteryl chloroformate as described in the Experimental Section. The reaction is schematically depicted in **Figure 1**. By the multiple purification steps performed, the impurities and unreacted starting materials have been completely removed from the product. Due to the balanced ratio between the hydrophilic PEI and lipophilic cholesterol, the prepared WSLP is well soluble in water. The average molecular weight of PEI was not provided and therefore, we had to determine it using dynamic light scattering (DLS) measurements as $M_w \approx 139 \pm 1$ kDa (Figure S1, Supporting Information). However, the same method was not suitable for the determination of the increased molecular mass of WSLP, because of the artefacts arising from the light scattering of some aggregates.

2.1.1. Determination of Critical Micelle Concentration

WSLP is able to behave like a surfactant and forms micelles in aqueous solutions thanks to its amphiphilic chemical structure.

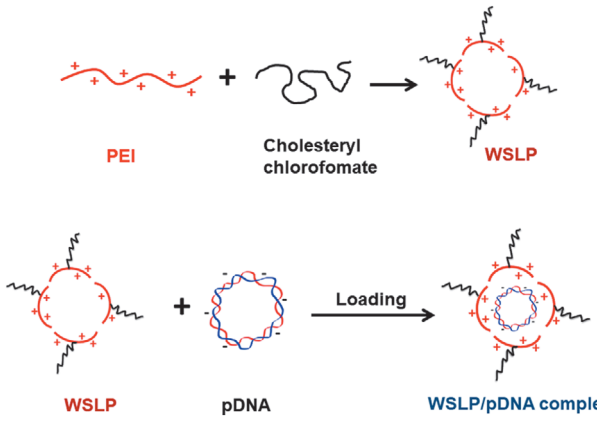

Figure 1. Schematic representation of the WSLP/pDNA complex formation.

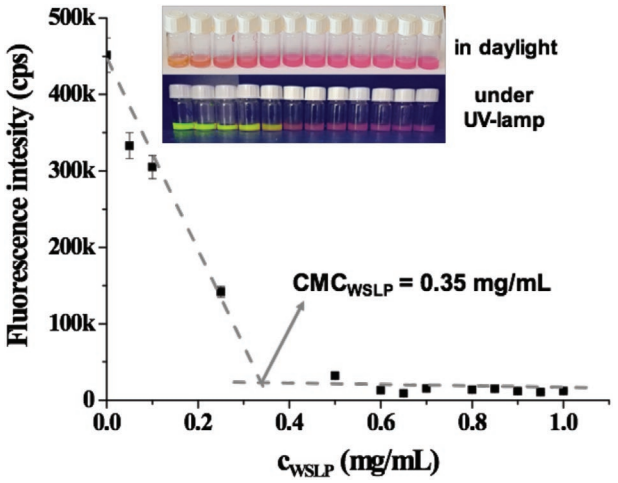

Figure 2. Representative determination of the CMC of WSLP by dye solubilization method using fluorescence spectroscopy (λ_{ex} = 490 nm, λ_{em} = 540 nm), with the photos of samples in daylight and under UV-lamp in the inset of the figure.

For the determination of critical micelle concentration (CMC), representing the concentration, above which the micelle formation occurs, fluorescent Eosin red indicator was used. The fluorescence of the dyes is rather sensitive to the chemical environment. The intensity of the fluorescence increases and the wavelength of the maximum intensity shifts in the presence of a number of surfactants.[36] At the same time, some multiple positively charged surfactants may quench the fluorescence.[37] It has also been reported that PEI is quenching the Eosin fluorescence due to the strong interaction of the negatively charged dye molecule with multiple positively charged surfactant.[38] Similarly, the increase of the WSLP concentration caused a decrease of the Eosin fluorescence intensity. As it can be seen in **Figure 2**, WSLP behaves as a quencher of the dye. Based on the measured data, it can be established that the polymer applied at higher concentration than CMC caused complete fluorescence quenching in contrast to the conventional monocationic surfactants, where the fluorescence of the dye starts to increase above of CMC.[39] The rapid decrease in the fluorescence intensity indicates the development of micelles, while the intensity does not change further upon completion of this process. The CMC of 0.35 ± 0.03 mg mL^{-1} was obtained by this method for the WSLP.

2.1.2. Particle Charge Detection

The WSLPs obtained by cholesterylation of low molecular weight PEI are usually characterized by nuclear magnetic resonance (NMR) and matrix-assisted laser desorption/ionization time-of-flight mass spectrometry (MALDI TOF MS) in terms of the molecular weight and cholesterylation extent.[35,40–47] These methods perform well with small and medium size molecules, but become of limited use for compounds with the molecular weight with several hundreds of thousands Da. The broadening effect of the NMR bands due to the slow molecular tumbling can already be experienced with the WSLP having $M_w > 10$ kDa,[35,46,47] while according to our knowledge no MS

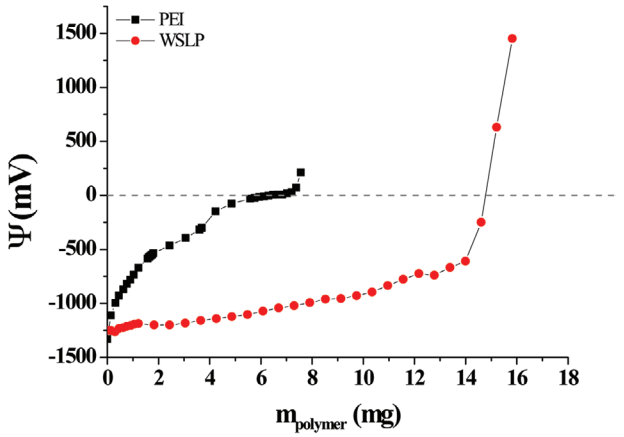

Figure 3. Titration of SDS with PEI or WSLP solutions for the detection of the charge neutralization point in a charge particle detection experiment, as described in the Experimental Section.

data are published for high molecular weight PEI or WSLP. Therefore, we were looking for a readily available simple method for checking the cholesterylation extent. Since cholesterylation or the modification in general, may affect the specific charge of the polymer both through the reaction with the amine groups and through increasing the molecular weight, such measurements could provide useful information, independently of the size of the polymer. The specific charge of the polymers was determined by the titration of sodium dodecyl sulfate (SDS) by PEI and WSLP, and checking the charge neutralization points. As it can be seen in **Figure 3**, the negative streaming potential continuously increased by the increase of the amount of the polymers. Based on the measured data, the charge compensation occurred upon adding of 6.5 mg PEI or 14.8 mg WSLP into the particle charge detector (PCD) cell. Knowing the applied amount of SDS, the specific charges of PEI and WSLP were calculated, to be q(PEI) = 15.38 mmol g^{-1} and q(WSLP) = 6.76 mmol g^{-1}, respectively. Using these data and the molecular weight of the initial PEI (Figure S1, Supporting Information), the protonated fraction of PEI can be estimated. The theoretically maximal specific charge of the applied PEI polymer is 23.22 mmol g^{-1}, suggesting that ≈66% of the nitrogens are protonated in PEI under the measurement conditions. This is in very good agreement with the published values in the literature for branched PEI molecules determined from acid–base titrations.[48,49]

It can also be concluded that the specific charge has decreased in the cholesterylation step. The ratio of q(WSLP)/q(PEI) is ≈0.44, meaning that the WSLP has 56% less specific charge than PEI. Since the specific charge, q depends on the molecular weight, M_w and the number of charges in a single molecule, n^+ the decrease of the specific charge may occur both by the increase of M_w and decrease of the number of the protonated nitrogens according to Equation (1).

$$q\left[\frac{\text{mmol}}{\text{g}}\right]=\frac{1}{M_w}n^+1000 \tag{1}$$

The cholesterylation occurs at more reactive primary amine groups which have to be deprotonated under the reaction conditions, but they might be protonated in a buffer solution at pH ≈ 7. An initial PEI molecule with M_w of 139 kDa contains 3227 nitrogens, out of which ≈2138 are protonated based on the measured specific charge. The increase of the M_w may play major role in the decrease of the specific charge of WSLP compared to PEI, if the number of protons at the nitrogens does not change as the consequence of the modification. In this case the increased M_w can be calculated from Equation (1), based on the specific charge value of the WSLP. This calculation yields ≈316.5 kDa as the new *M*w. This molecular weight is the sum of the original 139 kDa of the PEI and the mass increase due to the cholesterylation, that is: 316 492 = 139 000 + x(449.11 − 35.45). Here, x is the number of the conjugated cholesteryl groups per a PEI polymer, which can be easily calculated to be x ≈ 429. This reveals that approximately 13% of the nitrogens have been cholesterylated. On the other hand, we also may carry out the calculation assuming that the charge on the new WSLP molecule is decreased by the number of the cholesteryl groups attached to the nitrogens of PEI. In this case Equation (1) will be used for the calculation of x in its following form:

$$6.76=\frac{1}{139000+x(449.11-35.45)}(2138-x)1000 \tag{1'}$$

From this, x ≈ 316 is obtained. Thus, ≈10% is suggested for the possible fraction of the cholesterylated nitrogens. The molecular weight of the synthesized copolymer is ≈269.7 kDa by this assumption. The real number of the attached cholesteryl groups might be between the above two values assuming that no further deprotonation of the WSLP is caused by the modification. This calculation provides closer estimates for the possible domains of important parameters such as the molecular weight and the charge content of the newly prepared polymer.

2.2. Condensation Efficiency of the Water-Soluble Lipopolymer

WSLP/pDNA complexes are usually prepared by adjusting the mass or N/P ratios. It has to be mentioned that the two types of preparations cannot be directly compared with each other. The N/P ratio is the ratio of the number of nitrogen atoms of WSLP and the number of the phosphorous atoms of plasmid DNA. The number of nitrogen atoms is obtained by dividing the molecular weight of the polymer with the molecular weight of the monomer (there is one N atom in a monomer) and P atoms are calculated as 2000× kb of the plasmid DNA. For this, the knowledge of the molecular weight, that is, the extent of the modification of PEI, as well as the protonation state of the polymer is essential. It is usually very difficult to determine these parameters precisely.

We optimized the loading efficiency of WSLP using pEGFP-N3 and pX458 plasmids within both the mass and the N/P ratios ranging from 1.25 to 20.0 as it is described in more detail in Chapter S1, Supporting Information. DNA loading ability of WSLP was monitored by agarose gel electrophoresis. The results on N/P ratio series are shown in **Figure 4**. On increase of the N/P ratio, free DNA could not be detected on agarose gel when the value of N/P ratio reached 5/1, confirming the effectiveness of condensation by the polymer. This is due to the fact that positively charged head groups of WSLP interact strongly with the

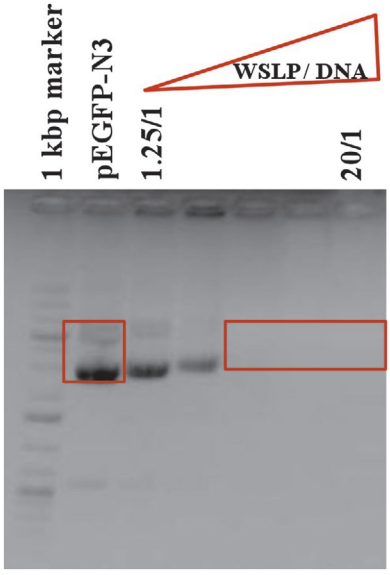

Figure 4. Agarose gel electrophoresis picture of naked pEGFP-N3 plasmid and WSLP/ pEGFP-N3 complexes formed by WSLP with the plasmid at N/P ratios 1.25, 2.5, 5, 10, and 20 in lanes 3–7, respectively.

negatively charged phosphate ions in the backbone of plasmid DNA independently of its nucleotide sequence. Nevertheless, the specific charges put the case more clearly, since the specific charge of the DNA which should be 3.24 mmol g^{-1}, can directly be compared with the specific charge of the polymer. At 5/1 N/P ratio the reaction mixture was constructed by mixing 1.00 μg of pDNA with 0.76 μg of WSLP. Based on the specific charges this corresponds to a positive/negative charge ratio of 5.14/3.24, that is, the total charge of the WSLP/pDNA complex is positive, while at N/P = 2.5/1 is still negative. This is in good agreement with the fact that the band of the DNA can be detected at N/P = 2.5/1 ratio on the agarose gel, although its mobility is less than that of the free DNA. At the same time the DNA band at N/P = 5/1 ratio does not appear. The mass ratio of 5/1 would correspond to a positive/negative charge ratio of 33.8/3.24, which means that this particle is already highly positively charged. Thus, by measuring the specific charge of the polymers the preparations using various types of ratios become comparable with each other.

2.3. Characterization of WSLP/DNA Complexes

Preparations of WSLP/pEGFP-N3 and WSLP/pX458 complexes with various composition ratios were characterized by DLS to determine the particle size and ζ-potential. The loading of plasmids into the polymer with defined colloidal and surface properties plays a major role in controlling stability, biodistribution, and intracellular fate of formulated plasmids. In contrast to the large size of naked DNA,[50] complex formation between WSLP and plasmid DNA resulted small-sized particles. For WSLP/pEGFP-N3 complexes, the mean particle size was in the range of 53.1–268.6 nm depending on the N/P ratio. ζ-potential of WSLP/DNA complexes increased with the increase of the charge ratio. At the N/P ratio of 2.5/1, it was −22.4 mV, but increased to +15.3 mV when formulated at N/P ratio of 20/1 as shown in **Table 1**. The size and ζ potential values for WSLP/pX458 complexes differ from the WSLP/pEGFP-N3 complexes as shown in **Table 2**.

Table 1. The average size and ζ-potential values of WSLP/pEGFP-N3 plasmid complexes at different N/P ratios.

N/P ratio	*d* [nm]	ζ-potential [mV]
1.25/1	53.1 ± 9.5	−22.4 ± 0.4
2.5/1	93.2 ± 9.2	−25.3 ± 0.2
5/1	138.8 ± 24.6	−20.3 ± 1.1
10/1	142.5 ± 14.8	+1.9 ± 0.2
15/1	163.8 ± 39.2	+12.3 ± 0.5
20/1	268.6 ± 19.2	+15.3 ± 1.3
WSLP	36.7 ± 3.5	+61.6 ± 0.4

The WSLP/pEGFP-N3 complexes were characterized by scanning electron microscopy (SEM) and transmission electron microscopy (TEM). The recorded images are shown in **Figure 5**. Both SEM and TEM detected the particle sizes being in good agreement with the values determined by DLS. The significant increase in size of the pDNA/WSLP nanoparticles (>100 nm; Figure 5D) in comparison with the WSLP itself (<50 nm; Figure 5C) is clearly demonstrated by TEM, supporting the successful condensation of the negatively charged pDNA by the cationic lipopolymer. Also, the pure WSLP in most cases showed fibrous structure on solid surfaces (e.g., copper grid) as can be also seen on the Figure 5C, while the morphology became nearly spherical-like upon complexation with DNA. The image shown in Figure 5D suggests a core-shell-like architecture of the pDNA/WSLP complex, which is assumed based on the different electron diffractions of the two components, due to their significantly distinct molecular weight. However, we could not unequivocally confirm such structure upon analyzing more particles (Figure 5E,F).

2.4. Cytotoxicity Assay

Since it is the major concern with many transfection protocols, we monitored the cytotoxicity of WSLP and WSLP/pEGFP-N3 complexes on A549 and HeLa cell lines after 24 and 48 h incubation at 37 °C using MTT cytotoxicity assays. According to the results shown in **Figure 6**, the polymer is only slightly toxic to the cells at 304 ng per well WSLP concentration. However, cell viability decreased significantly upon increase of the WSLP concentration, which indicates a remarkable dose-dependence of cytotoxicity. We have also checked the cytotoxicity of the WSLP/pEGFP-N3 preparations as a function of the ratio of the two components. The average cell viabilities upon treatment with

Table 2. The average size and ζ-potential values of WSLP/pX458 plasmid complexes at different N/P ratios.

N/P ratio	*d* [nm]	ζ-potential [mV]
2.5/1	61.0 ± 4.7	−19.7 ± 4.9
5/1	63.1 ± 7.6	−3.2 ± 3.3
10/1	133.2 ± 5.2	+23.1 ± 4.5
20/1	131.9 ± 3.5	+28.9 ± 1.7

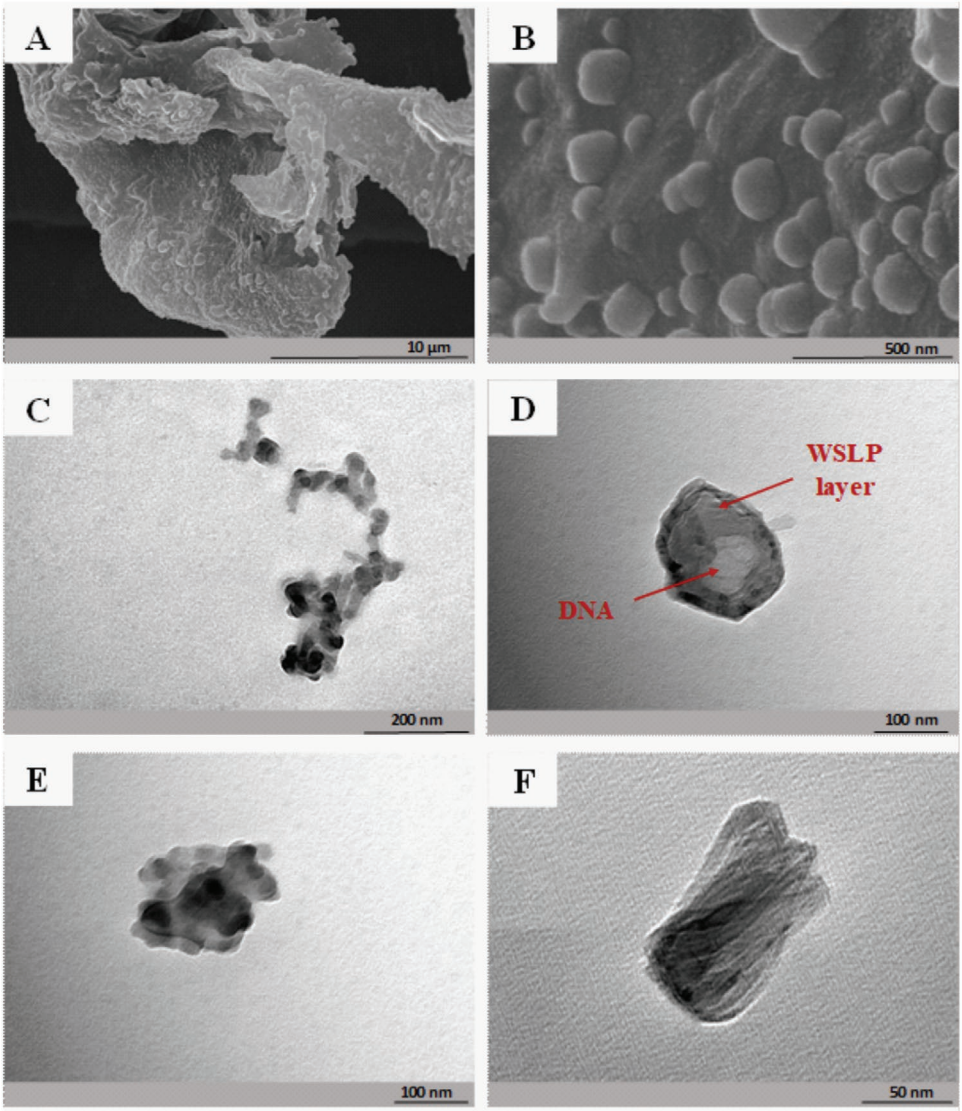

Figure 5. A,B) SEM images of the WSLP/pEGFP-N3 complex using 5/1 mass ratio preparations under different magnifications. C) TEM image of the WSLP itself. D–F) TEM images of selected WSLP/pEGFP-N3 nanoparticles from the 10/1 N/P ratio preparation.

WSLP/pEGFP-N3 of increasing N/P ratios from 5 to 20, decreased from ≈84% to ≈36% for A549 cells, and from ≈80% to ≈8%, for HeLa cells after 24 h. It is important to note that upon association of the WSLP with the pDNA, the toxic effect did not increase compared to the WSLP itself. Cytotoxicity was reasonably low even at 10/1 N/P ratio for A549 cells, nevertheless it depended remarkably on the type of the applied cell. The microscopic images of the cells treated with WSLP/pEGFP-N3 complexes show that the majority of the cells are destroyed by the excess of WSLP (Figure S3, Supporting Information).

In Figure S2, Supporting Information, we compared the cytotoxicity of the preparations based on the mass and N/P ratios. The average cell viability decreased quickly upon treatments with WSLP/pEGFP-N3 complexes of increasing mass ratios from 5 to 20, while adjusting the N/P ratios between 5 and 20 affected only slightly the viability of human A549 cells. We concluded that during the preparation of the WSLP/pDNA complexes the mass and N/P ratios may cause significantly different effects and the comparative evaluation of the results can only be accomplished considering the specific charges as described above. From these results, we can conclude that the minimization of the excess positive charges shall be targeted to decrease the toxic effect of the WSLP upon DNA delivery to the cells.

We have also checked the toxic effect of the WSLP preparations in comparison with the starting HMW PEI, as well as with the commercial standard transfection reagent Lipofectamine 3000 (Thermo Fisher Scientific). The latter has similar toxicity and transfection characteristics as the PEI25K often applied as a standard.[51–53] The results are included in Figure S4, Supporting Information, showing that original HMW PEI is extremely toxic to the cells, in agreement with the literature data, demonstrating the increasing toxicity by increasing M_w.[15] On the other hand, upon cholesterylation of this HMW PEI, the resulted WSLP performs similarly to Lipofectamine.

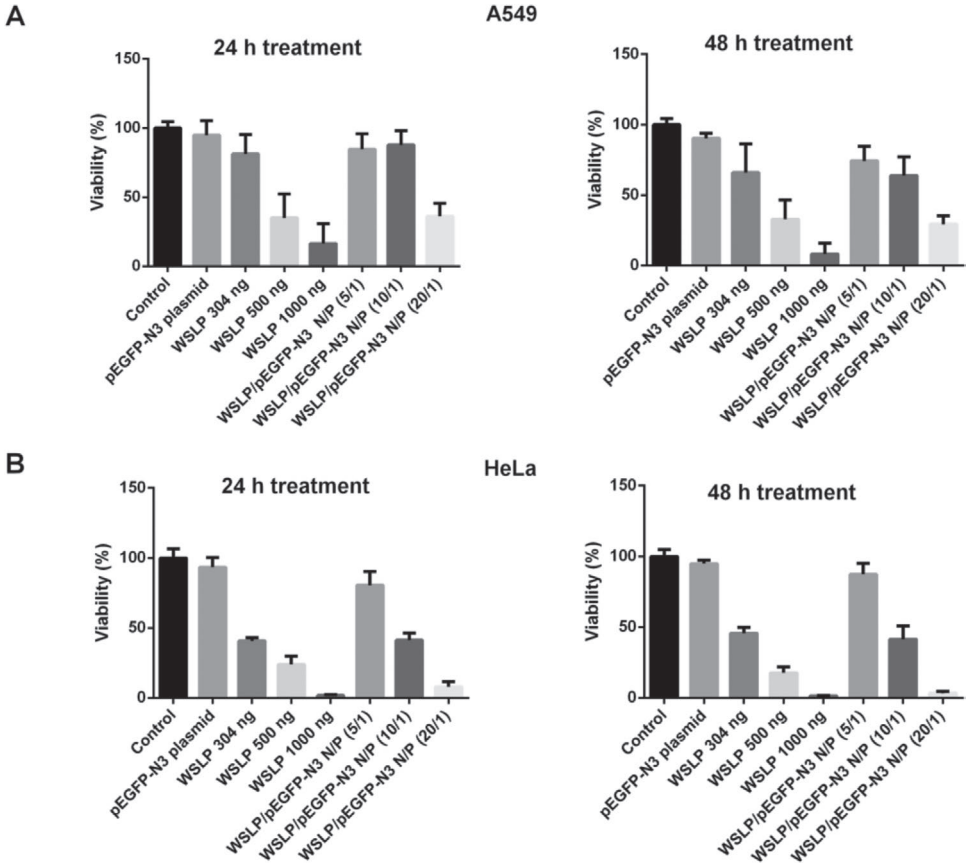

Figure 6. In vitro cytotoxicity analysis of naked DNA, WSLP, and WSLP/pEGFP-N3 at various N/P ratios on A) A549 and B) HeLa cells using MTT assay. Viability of the naked DNA, WSLP, and WSLP/pEGFP-N3 treated cells was normalized to the untreated controls.

2.5. In Vitro Transfection

The transfection efficiency of WSLP/pEGFP-N3 complexes at various N/P ratios was determined in A549 and HeLa cells as shown in **Figure 7** and Figure S5, Supporting Information. According to the results of flow cytometry, the most efficient transfection was achieved at 20/1 N/P ratio in both cell lines. This can be surprising, since the MTT assays revealed that the 20/1 N/P ratio preparation caused more significant cytotoxicity than the preparations with lower N/P ratios. This effect has already been reported multiple times in the literature.[40] It may be explained by the fact that the stably transfected

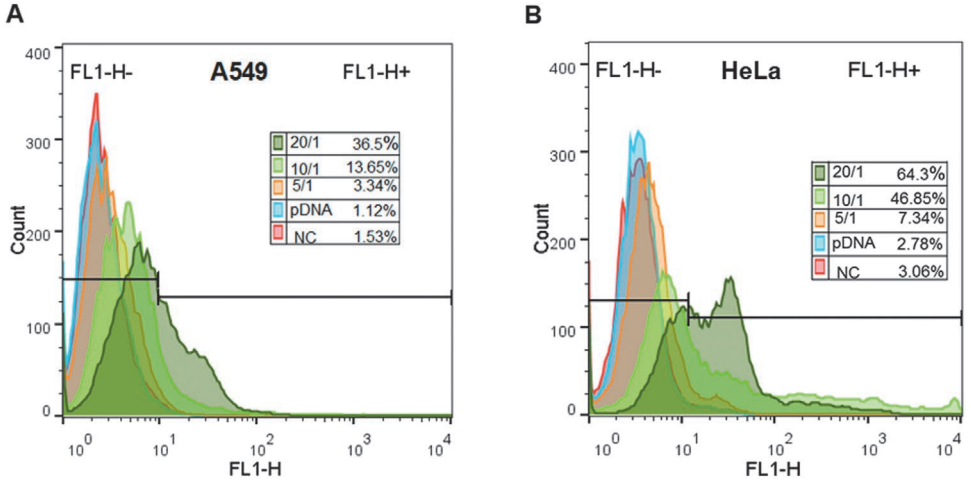

Figure 7. Flow cytometric analysis of in vitro transfection efficiency. A) A549 and B) HeLa cells were transfected with WSLP/pEGFP-N3 complexes of various N/P ratios.

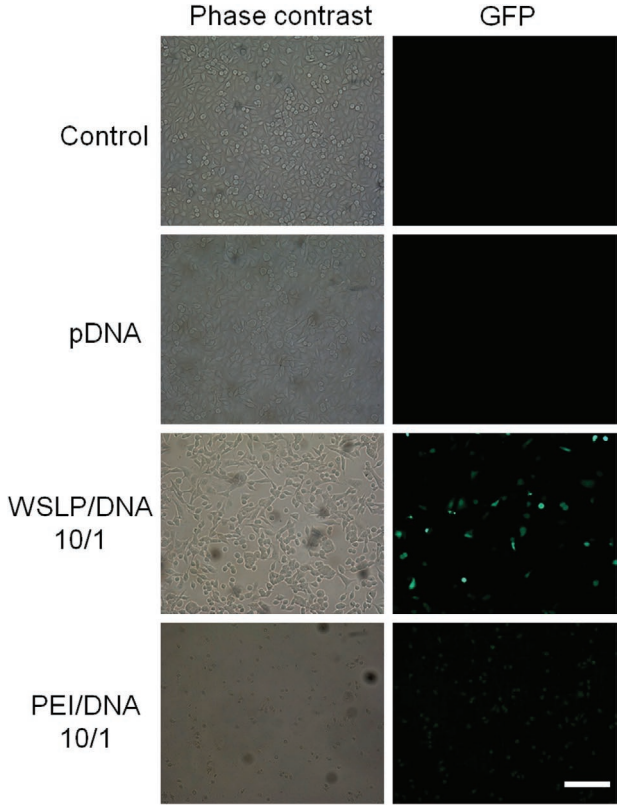

Figure 8. Fluorescence microscopic images of A549 cells transfected by WSLP/pEGFP-N3 complexes at 10/1 N/P ratio after 48 h incubation time. PEI was used for comparison. The scale bar represents 500 μm and it is same for all images in this figure.

cells may efficiently proliferate during the incubation after the transfection procedure. Indeed, the transfection efficiency reached 36.5% in the case of A549 cells and 64.3% in the case of HeLa cells. These values render this type of WSLP promising for its applicability in in vivo transfection experiments after the required optimization is achieved to reduce the cytotoxic side-effect.

The transfection efficiency using the pX458 plasmid was checked with WSLP, and also including the starting HMW PEI, as well as the commercial standard transfection reagent Lipofectamine 3000 (Thermo Fisher Scientific) for comparison. The results included in Figure S6, Supporting Information, demonstrated the high transfection efficiency of highly cytotoxic PEI, in agreement with the literature data.[20] The transfection efficiency of the WSLP at N/P 10/1 ratio was similar to Lipofectamine. It is worth mentioning that the success of the transfection experiments with the large pX458 plasmid (9289 base pairs; Figure S6, Supporting Information), was similar to that of pEGFP-N3 plasmid (4729 base-pairs; Figure 7), most probably due to the efficient condensation of the DNA in both cases.

As another proof of the successful gene delivery using WSLP/DNA complexes, the direct visualization of gene expression of EGFP in A549 cells was confirmed using an inverted fluorescent microscope. **Figure 8** clearly indicates that GFP expression is more intense in cells transfected with the WSLP/pDNA than with PEI/pDNA complexes at 10/1 N/P ratio. The fluorescence is more diffuse when PEI was applied instead of WSLP, which can be easily explained by the phase contrast images, showing that PEI is much more toxic than WSLP.

GFP expression was also observed using fluorescence microscopy after the transfected A549 cellular nuclei were stained with Hoechst 33432 fluorescent dye. Hoechst 33432 is a cell permeable fluorescent nuclear stain that specifically binds to DNA. In fluorescent microscopic experiments such nuclear stains are used to detect intactness of the nucleus, to assess the localization or colocalization of fluorescently labeled cellular proteins, and to count total number of cells. The results revealed that more GFP was expressed using WSLP as transfection agent than with PEI (Figure S7, Supporting Information) and the high GFP fluorescence intensity was colocalized with the Hoechst fluorescence. In other words, the WSLP/DNA complexes showed higher intracellular distribution than PEI/DNA.

3. Conclusion

In this work an EGFP (pEGFP-N3) and a CRISPR/Cas9 (pX458) carrier plasmid DNA both expressing the EGFP fluorescent protein for detectability of transfection were efficiently condensed by a water soluble lipopolymer. The WSLP consisted of positively charged hydrophilic PEI functionalized with lipophilic cholesterol. The cholesterylation was efficient, in average ≈10% of the PEI nitrogens were reacted. This kind of modification of a cytotoxic high molecular weight PEI seems to be promising, since it retains the positive charges for strong interaction with DNA, while decreasing the toxicity of the preparation. The interaction between the lipopolymer and DNA was monitored by agarose gel electrophoresis, which clearly showed the lack of the free DNA at 5/1 and higher N/P ratios of the WSLP and DNA. The size of these nanoparticles was close to 100 nm. Electron microscopy showed that the DNA is condensed with the cationic WSLP, being important for the protection of the carried DNA against DNA degrading and damaging agents. Although previously it was found that the high molecular weight PEI is toxic to the cells,[17] we have found that our WSLP and the WSLP/DNA adducts did not show significant toxicity at concentrations of ≈150 ng per well. However, the toxicity was dose and cell-line dependent. We could efficiently transfect A549 and HeLa cells under the applied conditions, which proved to be less efficient for Lipofectamine 3000 standard transfection reagent similarly to the data found in the literature for small molecular weight PEI-based WSLP or similar gene carrier systems.[40,54] Nevertheless, the results indicate that the optimization of high molecular weight cationic polymers, such as the PEI, for gene delivery leads through the chemical modification of the polymer, and the minimization of the positive charge excess, needed to efficiently cross the membrane. Similar direction of developing the new gene carriers are presented by studies using the minimum amount of high molecular weight PEI supplemented with low molecular weight PEI for increased transfection efficiency,[55] or regulating the charge of the polymer by optimizing the pH during the transfection.[56] In addition, the combination of various agents such as amphiphilic copolymers or proteins, to obtain carriers with

multifarious properties will lead to fine-tuning of the polymeric gene delivery systems.[57,58]

4. Experimental Section

Materials: PEI (30% m/v in water) was purchased from Tokyo Chemicals, trimethylamine ($(C_2H_5)_3N$, 99%), methylene chloride (CH_2Cl_2, anhydrous, ≥99.8%), cholesteryl chloroformate ($C_{28}H_{45}ClO_2$, 95%), diethyl ether ($(CH_3CH_2)_2O$, anhydrous, ≥99.7%) were purchased from Sigma, and acetone (CH_3COCH_3, ≥99%) was manufactured by Molar. The stock solutions were freshly prepared using MQ (Millipore, Milli-Q Integral3) ultrapure water (18.2 MΩ cm at 25 °C) in every case. The pSpCas9(BB)-2A-GFP (pX458) and the pEGFP-N3 plasmids were purchased from Addgene. The Qiagen Plasmid Mini Kit was purchased from Qiagen. The MTT reagent (3-[4,5-dimethylthiazol-2-yl]-2,5-diphenyltetrazolium bromide), penicillin, and streptomycin were obtained from SERVA. Dulbecco's modified eagle medium (DMEM) fetal bovine serum and L-glutamine were purchased from Lonza.

Synthesis and Purification of the Water-Soluble Lipopolymer: The synthesis and the purification of WSLP were carried out based on the description in the literature[40] as shown schematically in Figure 1. 3 g of PEI (10 mL PEI solution) was mixed with 10 mL ice-cold methylene chloride and 100 µL trimethylamine. Then 1 g of cholesteryl chloroformate was added to 5 mL chilled methylene chloride and this solution was slowly mixed with the PEI solution. The mixture was stirred at 0 °C using 800 rpm for 12 h resulting in a pale yellow solid product. The synthesized WSLP was purified by the following steps. First, the product was completely dried by rotary evaporation (IKA, RV 3 evaporator), then the powder was dissolved into 50 mL of 0.1 M HCl, and an extraction was repeated three times using 50 mL methylene chloride. For the removal of the large aggregates, vacuum filtration was applied by standard P3 glass and paper filters with 16–40 and 3–5 µm pore size, respectively. The filtered liquid was concentrated by rotary evaporation (50 °C, 2 h) then the WSLP was precipitated by acetone and the filtration was repeated as described above. Finally, the solid WSLP was obtained by freeze drying (Christ Alpha, 1 2 LD dryer) for 1 day.

Determination of the Critical Micellar Concentration of the Water-Soluble Lipopolymer: The CMC of the WSLP was determined by following the fluorescence of the Eosin red indicator in the presence of an increasing amount of WSLP. Since the synthesized WSLP polymer had both a positively charged hydrophilic (imine moieties) and a hydrophobic (cholesterol) side chain, it was able to show surfactant-like behavior such as micelle formation. For the measurements, 5 mL of 20 µM Eosin red was mixed with 5 mL WSLP solution of varying concentrations between 0 and 1 mg mL^{-1}. The fluorescence spectra were recorded by a Horiba, Jobin Yvon Fluoromax-4 spectrofluorometer using 1 cm quartz cuvette. The excitation wavelength was 490 nm, the emission maximum was 540 nm using 3–3 nm slits. The measurement data were analyzed with the Origin 8.5 software.

Particle Charge Measurements: The charge of the initial PEI and the synthesized WSLP was determined at pH = 7.4 using a PCD-04 type of Mütek Particle Charge Detector. Namely, 10 mL of 0.01 M SDS solution in the PCD cell was titrated separately with 25.2 mL of 0.3 mg L^{-1} PEI and 26 mL of 0.6085 mg L^{-1} WSLP in 300 and 1000 µL steps, respectively. The streaming potential was recorded 30 s after each step. The measurements were analyzed and the charge neutralization point was appointed based on the sigmoidal shape of the charge titration curve. The possible extent of the PEI protonation, the cholesteryl substitution, and the presumable molecular weight of the synthesized WSLP were also calculated.

Amplification and Purification of the Plasmid DNA: Competent *Escherichia coli* DH5α cells were transformed by pX458 and pEGFP-N3 plasmids and cultured in lysogeny broth media containing 0.1 mg mL^{-1} ampicillin. The plasmids were then purified by Plasmid Mini Kit (Qiagen) and subsequent precipitation with polyethylene-glycol (PEG6000). The concentration of the DNA was determined by a NanoDrop Lite spectrophotometer (Thermo Fisher Scientific). Purity of the DNA samples was assessed prior to loading into the lipopolymer.

DNA Condensation by WSLP: WSLP and pDNA were mixed at various compositions in sterilized water and incubated for 15–20 min at room temperature to allow complex formation between the lipopolymer and the plasmid DNA. The samples were subjected to electrophoresis in 1% m/v agarose gel in 1× tris-acetic acid-EDTA buffer at 100 V until the 1× orange blue loading dye ran through 80% of the gel. The GeneRuler 1 kb Plus DNA Ladder (Thermo Fisher Scientific) served as a DNA size marker. Ethidium bromide was used for DNA visualization. The plasmid DNA was analyzed by an UviDoc (UviTec Ltd.) gel documentation system.

Particle Size and Zeta Potential Measurements: The hydrodynamic diameter and the ζ-potential of the WSLP itself and the WSLP/pDNA complexes, as well as, the molecular weight of the initial lipopolymer were determined by dynamic and static light scattering (DLS and SLS, respectively) using a Malvern Zetasizer Nano ZS ZEN 4003 apparatus equipped with an He–Ne laser ($\lambda = 633$ nm) at 25 ± 0.1 °C. The refractive index gradient was calculated by a Mettler Toledo Excellence RM50 refractometer. The morphology of the initial WSLP and the WSLP/pDNA complexes was also examined by electron microscopy techniques. The SEM pictures were recorded by a Hitachi S-4700 Field Emission Scanning Electron Microscope using 20 kV accelerating voltage. For the TEM images, a Jeol JEM-1400plus equipment (Japan) with 120 keV accelerating voltage was applied and the samples were dropped on the surface of formvar-coated grid. The pictures were analyzed by ImageJ software.

The average molecular weight was determined by DLS measurements based on the Debye plot (KC/R as a function of the C concentration) using the Zimm equation (Equation [2]). The slope of the fitting provided the second virial coefficient ($2A_2$) and the intercept yielded the reciprocal of the molecular weight ($1/M_w$).

$$\frac{KC}{R} = \frac{1}{M_w P} + 2A_2 C \tag{2}$$

where K is a constant dependent on the sample dn/dc, C is the sample concentration in g mL^{-1}, R is the Rayleigh ratio (the ratio of scattered light intensity to incident light intensity), M_w is the average molecular weight, and A_2 is the second virial coefficient. P is an angular dependent term (by default, assumed to be 1 for small molecules <15 nm radius).

Cell Culture: A549 human lung cancer cells and HeLa cervical adenocarcinoma cells were obtained from the American Type Culture Collection (ATCC, USA). Cells were maintained in DMEM (Lonza) supplemented with 10% fetal bovine serum (FBS), L-glutamine (2 mM), penicillin (100 IU mL^{-1}), and streptomycin (50 µg mL^{-1}) in a humidified atmosphere containing 5% CO_2 at 37 °C.

Cytotoxicity Assay: The cytotoxicity of WSLP/pDNA complexes prepared according to the mass and N/P ratios was determined by MTT assay. A549 and HeLa cells were seeded at 5000 cells per well density in 96-well plates and incubated for 24 h at 37 °C to reach 70% confluence. Then the medium was removed and the WSLP, WSLP/pEGFP-N3 complexes were added to the cells in serum-free DMEM. Following the incubation at 37 °C for 24 and 48 h, the medium was removed and the cells were washed with phosphate buffered saline (PBS). Cell viability was assessed by adding the MTT reagent prepared in serum-free DMEM to a final concentration of 0.5 mg mL^{-1}. After incubation (1 h at 37 °C), the media was removed and 100 µL dimethyl sulfoxide (Serva Electrophoresis GmbH) was added to dissolve the formazan crystals. The absorbance was measured at 570 nm using Synergy HTX plate reader (BioTek-Hungary). Data were analyzed by GraphPad Prism 7 software (GraphPad Software; San Diego, CA, USA), where untreated cells served as the control.

In Vitro Transfection: A549 and HeLa cells were seeded in 6-well tissue culture plates at a density of 2×10^5 cells per well in 10% FBS-containing DMEM and were left to grow. After the cells reached 70% confluency, the medium was replaced with serum-free DMEM and the cells were transfected with WSLP/pEGFP-N3 complexes at DNA concentration of

2.5 µg per well. After 24 h incubation at 37 °C, the medium was replaced by a DMEM medium supplemented with 10% FBS, L-glutamine, penicillin, and streptomycin in concentrations described above. The cells were incubated for an additional 48 h, then were trypsinized, washed, and resuspended in PBS. The transfection efficiency was detected by flow cytometry using FACSCalibur platform via quantification of EGFP fluorescence. The analysis of the fluorescence-activated cell sorting data was performed with FlowJo and Graphpad softwares.

Fluorescence Microscopy: To validate the results of the flow cytometry experiments, the transfection efficiency by fluorescence microscopy was assessed as well. For this, A549 cells were seeded on glass coverslips (VWR), placed into the wells of a 24-well plate and were left to grow. When the cells reached about 70% confluence the culture medium was replaced to serum-free DMEM and the cells were transfected with WSLP/pEGFP-N3 and with PEI/pEGFP-N3 complexes at 10/1 N/P ratio with DNA concentration of 0.75 µg per well. After 24 h the cells were washed with PBS and were left to grow for 48 h in FBS-containing culture medium. Cells were visualized by OLYMPUS BX51 fluorescence microscope and the photos were taken by Olympus DP70 camera (Olympus, Tokyo, Japan) with or without staining with 3.25 µм Hoechst 33432 (Sigma-Aldrich) dye for 30 min.

Supporting Information

Supporting Information is available from the Wiley Online Library or from the author.

Acknowledgements

This work was supported by the Hungarian National Research, Development, and Innovation Office (GINOP-2.3.2-15-2016-00038 and NKFIH K_16/120130). H.A.H.A.E. is a Stipendium Hungaricum Ph.D. fellow supported also by Cultural Affairs and Mission Sector in Egypt. This work was supported by the János Bolyai Research Fellowship of the Hungarian Academy of Sciences (E.C.). The Ministry of Human Capacities, Hungary grant TUDFO/47138-1/2019-ITM is acknowledged.

Conflict of Interest

The authors declare no conflict of interest.

Keywords

drug delivery systems, high molecular weight, hydrophilic polymers, modification, specific charge

Received: February 6, 2020
Revised: April 15, 2020
Published online: May 25, 2020

[1] S. D. Li, L. Huang, *Gene Ther.* **2006**, *13*, 1313.
[2] N. Nayerossadat, P. Ali, T. Maedeh, *Adv. Biomed. Res.* **2012**, *1*, 27.
[3] L. Jin, X. Zeng, M. Liu, Y. Deng, N. He, *Theranostics* **2014**, *4*, 240.
[4] Y. K. Sung, S. W. Kim, *Biomater. Res.* **2019**, *23*, 8.
[5] G. Shim, D. Kim, G. T. Park, H. Jin, S. Suh, Y. Oh, *Acta Pharmacol. Sin.* **2017**, *38*, 738.
[6] S. D. Li, L. Huang, *J. Controlled Release* **2007**, *123*, 181.
[7] W. Wang, W. Li, N. Ma, G. Steinhoff, *Curr. Pharm. Biotechnol.* **2013**, *14*, 46.
[8] H. Yin, R. L. Kanasty, A. A. Eltoukhy, A. J. Vegas, J. R. Dorkin, D. G. Anderson, *Nat. Rev. Genet.* **2014**, *15*, 541.
[9] R. Mout, M. Ray, Y.-W. Lee, F. Scaletti, V. M. Rotello, *Bioconjugate Chem.* **2017**, *28*, 880.
[10] R. Rai, S. Alwani, I. Badea, *Polymers* **2019**, *11*, 745.
[11] A. Jafari, N. Rajabian, G. Zhang, M. A. Mohamed, P. Lei, S. T. Andreadis, B. A. Pfeifer, C. Cheng, *Materials* **2020**, *13*, 898.
[12] P. Campeau, P. Chapdelaine, B. Massie, J. P. Tremblay, *Gene Ther.* **2001**, *8*, 1387.
[13] M. E. Martin, K. G. Rice, *AAPS J.* **2007**, *9*, E18.
[14] A. Bansal, Himanshu, *Nanosci. Nanotechnol.-Asia* **2019**, *9*, 4.
[15] A. P. Pandey, K. K. Sawant, *Mater. Sci. Eng., C* **2016**, *68*, 904.
[16] A. Kichler, C. Leborgne, E. Coeytaux, O. Danos, *J. Gene Med.* **2001**, *3*, 135.
[17] U. Lungwitz, M. Breunig, T. Blunk, A. Göpferich, *Eur. J. Pharm. Biopharm.* **2005**, *60*, 247.
[18] S. Patnaik, K. C. Gupta, *Expert Opin. Drug Delivery* **2013**, *10*, 215.
[19] X. Wang, D. Niu, C. Hu, P. Li, *Curr. Pharm. Des.* **2015**, *21*, 6140.
[20] W. T. Godbey, K. K. Wu, A. G. Mikos, *J. Controlled Release* **1999**, *60*, 149.
[21] M. L. Forrest, J. T. Koerber, D. W. Pack, *Bioconjugate Chem.* **2003**, *14*, 934.
[22] Y. B. Lim, S. M. Kim, H. Suh, J. S. Park, *Bioconjugate Chem.* **2002**, *13*, 952.
[23] D. Jiang, A. K. Salem, *Int. J. Pharm.* **2012**, *427*, 71.
[24] J. Wang, B. Dou, Y. Bao, *Mater. Sci. Eng., C* **2014**, *34*, 98.
[25] Z. F. Zhang, C. H. Yang, Y. Duan, Y. Wang, J. Liu, L. Wang, D. Kong, *Acta Biomater.* **2010**, *6*, 2650.
[26] Z. Liu, Z. Zhang, C. Zhou, Y. Jiao, *Prog. Polym. Sci.* **2010**, *35*, 1144.
[27] Y. Zhu, Y. X. Wang, Q. L. Hu, J. C. Shen, *Mater. Sci. Eng., C* **2009**, *29*, 1066.
[28] Z. Salmasi, W. T. Shier, M. Hashemi, E. Mahdipour, H. Parhiz, K. Abnous, M. Ramezani, *Eur. J. Pharm. Biopharm.* **2015**, *96*, 76.
[29] Q. F. Zhang, C. R. Luan, D. X. Yin, J. Zhang, Y. H. Liu, Q. Peng, Y. Xu, X. Q. Yu, *Polymers* **2015**, *7*, 2316.
[30] Y. S. Siu, L. Li, M. F. Leung, K. L. D. Lee, P. Li, *Biointerphases* **2012**, *7*, 16.
[31] L. Wu, J. Xie, T. Li, Z. Mai, L. Wang, X. Wang, T. Chen, *R. Soc. Open Sci.* **2017**, *4*, 170822.
[32] D. G. Abebe, R. Kandil, T. Kraus, M. Elsayed, O. M. Merkel, T. Fujiwara, *Macromol. Biosci.* **2015**, *15*, 698.
[33] P. Lv, C. Zhou, Y. Zhao, X. Liao, B. Yang, *Carbohydr. Polym.* **2017**, *168*, 103.
[34] S. Qiu, R. Granet, J. P. Mbakidi, F. Bregier, C. Pouget, L. Micallef, T. Sothea-Ouk, D. Y. Leger, B. Liagre, V. Chaleix, V. Sol, *Bioorg. Med. Chem. Lett.* **2016**, *26*, 2503.
[35] M. Monajati, S. Tavakoli, S. S. Abolmaali, G. Yousefi, A. Tamaddon, *BioImpacts* **2018**, *8*, 241.
[36] S. Acharya, B. Rebery, *Arabian J. Chem.* **2009**, *2*, 7.
[37] R. Sharma, A. Kamala, R. K. Mahajan, *RSC Adv.* **2016**, *6*, 71692.
[38] J. Liang, X. Deng, K. Tan, *Spectrochim. Acta, Part A* **2015**, *150*, 772.
[39] A. Fluksman, O. Benny, *Anal. Methods* **2019**, *11*, 3810.
[40] S. O. Han, R. I. Mahato, S. W. Kim, *Bioconjugate Chem.* **2001**, *12*, 337.
[41] D. Y. Furgeson, W. S. Chan, J. W. Yockman, S. W. Kim, *Bioconjugate Chem.* **2003**, *14*, 840.
[42] D. Wang, A. S. Narang, M. Kotb, A. O. Gaber, D. D. Miller, S. W. Kim, R. I. Mahato, *Biomacromolecules* **2002**, *3*, 1197.
[43] R. I. Mahato, M. Lee, S. Han, A. Maheshwari, S. W. Kim, *Mol. Ther.* **2001**, *4*, 130.
[44] S. Bhattacharya, A. Bajaj, *Biochim. Biophys. Acta* **2008**, *1778*, 2225.
[45] A. Bajaj, P. Kondaiah, S. Bhattacharya, *Bioconjugate Chem.* **2008**, *19*, 1640.

[46] D. R. Holycross, M. Chai, *Macromolecules* **2013**, *46*, 6891.
[47] A. Concellón, S. Hernández-Ainsa, J. Barberá, P. Romero, J. L. Serrano, M. Marcos, *RSC Adv.* **2018**, *8*, 37700.
[48] D. R. Chang, S. Harden, N. Loverro, *J. Macromol. Sci., Part A: Pure Appl. Chem.* **1986**, *23*, 801.
[49] S. Kobayashi, K. Hiroishi, M. Tokunoh, T. Saegusa, *Macromolecules* **1987**, *20*, 1496.
[50] Y. B. Lim, S. O. Han, H. U. Kong, Y. Lee, J. S. Park, B. Jeong, S. W. Kim, *Pharm. Res.* **2000**, *17*, 811.
[51] N. Ryu, M.-A. Kim, D. Park, B. Lee, Y.-R. Kim, K.-H. Kim, J.-I. Baek, W. J. Kim, K.-Y. Lee, U.-K. Kim, *Nanomedicine* **2018**, *14*, 2095.
[52] S. Guo, Y. Huang, Q. Jiang, Y. Sun, L. Deng, Z. Liang, Q. Du, J. Xing, Y. Zhao, P. C. Wang, A. Dong, X.-J. Liang, *ACS Nano* **2010**, *4*, 5505.
[53] A. Swami, R. K. Kurupati, A. Pathak, Y. Singh, P. Kumar, K. C. Gupta, *Biochem. Biophys. Res. Commun.* **2007**, *362*, 835.
[54] L. Zhang, P. Wang, Q. Feng, N. Wang, Z. Chen, Y. Huang, W. Zheng, X. Jiang, *NPG Asia Mater.* **2017**, *9*, e441.
[55] Z. Dai, T. Gjetting, M. A. Mattebjerg, C. Wu, T. L. Andresen, *Biomaterials* **2011**, *32*, 8626.
[56] H. C. Kang, O. Samsonova, S.-W. Kang, Y. H. Bae, *Biomaterials* **2012**, *33*, 1651.
[57] B. Rasolonjatovo, N. Illy, V. Bennevault, J. Mathé, P. Midoux, T. Le Gall, T. Haudebourg, T. Montier, P. Lehn, B. Pitard, H. Cheradame, C. Huin, P. Guégan, *Macromol. Biosci.* **2020**, *20*, 1900276.
[58] D.-E. Liu, J. An, C. Pang, X. Yan, W. Li, J. Ma, H. Gao, *Macromol. Biosci.* **2019**, *19*, 1800359.